International Journal of Computer Science and Applications,
©Technomathematics Research Foundation
Vol. 13, No. 2, pp. 45 – 60, 2016

A NOVEL NEURAL NETWORKS-BASED TEXTURE IMAGE PROCESSING ALGORITHM FOR ORANGE DEFECTS CLASSIFICATION

GIACOMO CAPIZZI

Dep. of Electrica,l Electronic and Informatics Engineering, University of Catania, Viale A. Doria 6, 95125 Catania, Italy
gcapizzi@diees.unict.it

GRAZIA LO SCIUTO

Dep. of Engineering, University of Roma Tre, Via della Vasca Navale 84, 00146 Roma, Italy
glosciuto@dii.unict.it

CHRISTIAN NAPOLI and EMILIANO TRAMONTANA

Dep. of Mathematics and Informatics, University of Catania, Viale A. Doria 6, 95125 Catania, Italy
napoli@dmi.unict.it, tramontana@dmi.unict.it

MARCIN WOŹNIAK

Institute of Mathematics, Silesian University of Technology, Kaszubska 23, 44-100 Gliwice, Poland
marcin.wozniak@polsl.pl

In this paper is proposed, implemented and evaluated a novel radial basis probabilistic neural network (RBPNN) based classification algorithm for classification fruit surface defects in color and texture of a very important fruit as orange. The proposed algorithm takes orange images as inputs then the texture and gray features of defect area are extracted by computing a gray level co-occurrence matrix and the defect areas are classified through an RBPNN-based classifier. The conducted experiments and the results reveal as the classification accuracy achieved is up to 88%.

Keywords: Co-occurrence Matrix; Texture Analysis; Pattern Recognition; Probabilistic Neural Network.

1. Introduction

In order to ensure the quality standard required in orange production lines, companies need trained people to inspect the fruits while they move in a conveyor belt. These experts classify oranges according to several categories based on visual features. However, for fast and precise quality standards, this approach is not competitive and sometimes unreliable. Therefore it is paramount to use an automatic system based on intelligent methods[Pukish, *et al.* (2015)], [Reiner and Wilamowski (2015)], [Horzyk (2015)], where dedicated methods will help on energy usage [Damasevicius, *et al.* (2013)]or by application of devoted methods will improve efficiency [Woźniak, *et al.*(2014c)], [Horzyk (2014)], [Woźniak and Połap (2015a)], [Napoli and Tramontana (2015b)].Artificial Intelligence (AI) can improve various processes over input images [Ferdowsi, *et al.* (2015)], [Kostadinov *et. al* (2015)] and assist in classification purposes

where computer systems are implemented to detect specific features over various types of input images[Korytkowski, *et al.*(2016)], [Woźniak *et. al* (2015d)], [Woźniak and Połap (2014a)], [Woźniak and Marszałek (2014b)].Several methods for distributed systems based on the applicability of the AI are reported in [Capizzi,*et al.*(2011)], [Bonanno,*et al.*(2014b)]. Moreover distributed systems can be positioned for optimal efficiency [Swiechowski and Mandziuk (2014)], [Walendzik and Mandziuk (2014)] and managed by intelligent agents that control actions of connected users [Połap et al. (2015a)], [Połap et al. (2015b)]. These solutions can be adapted to fruit classification purposes.The aim of this paper is to investigate the applicability of the AI methods based on soft computing for detection of external defects of the fruits in multi agent systems. Wen and Tao developed a near-infrared vision system for automatic apple defect inspection, see [Wen and Tao (2000)], while some recent advances in feature extraction for images and biometrics are reported in [Kubanek, *et. al.* (2015)].Zion et al. introduced a computerized methodto detect the bruisesofJonathan, Golden Delicious, and Hermon apples from magnetic resonance images by threshold technique.The algorithm was only able to discriminate between all-bruised and non- bruised apples and was not applicable to on-line detection. Pla and Juste presented a thinning algorithm to discriminate between stem and body of the apples on monochromatic images. However, the task of classifying the calyx and defected parts in real-time was missing. Yang and Marchant used the 'flooding' algorithm for initial segmentation and 'snakes' algorithm for refining the boundary of the blemishes on the monochromatic images of apples. Miller et al. in [Miller,*et. al.* (1998)] compared differentneural network models for detection of blemishes of various kinds of apples by their reflectance characteristics.

From the said research, and according to the current literature, we can conclude that Multi-Layer Back Propagation (MLBP) gives proper recognition rates and also that increased complexity of the neural network system did not yield to better results. Leemans, segmented defects of 'Golden Delicious' apples by a pixel-wise comparison method between the chromatic (RGB) values of the related pixel and the color reference model. The local and global approaches of comparison were effective, but more research was needed. In his further research work, Leemans [Leemans, *et al.* (1998)] used a Bayesian classification method for pixel-wise segmentation on chromatic images of 'Jonagold' apples. Machine vision systems are successfully used for recognition of greenhouse cucumber using computer vision [Zhang, *et al.* (2007)]. A method for the classification and gradation of different grains (for a single grain kernel) such as groundnut, Bengal gram, Wheat etc., is described in [Savakarand Anami (2009)]. The effect of foreign bodies on recognition and classification of food grains is given in [Anami, *et al.* (2009)]. Some researchers have used a neural network approach to the color grading ofapples [Nakano (1997)]. All these studies show that it is hard to define geometric or spectral properties for the fruit skin.

Most of the industry treatments such as washing and packing are highly automated, while the most important verification steps (e.g., inspection and grading in quality) are still performed manually, around the world.For this reason, we propose an efficient classifier based on fruit skin texture analysis.

A new automatic classifier of oranges defects based on co-occurrence matrix and probabilistic neural networks is presented in the following sections.

Orange is an important fruit of Mediterranean countries and it is well-known for its considerable anti-microbial, anti-viral, potent anti-oxidant properties. High-quality products are the basis for the success in today's highly competitive market. Currently, manual inspection is being used in order to determine the orange quality. The increasing demand for quality assurance requires simple and reliable sorting methods. The use of computer vision systems enables the detection of external quality defects.

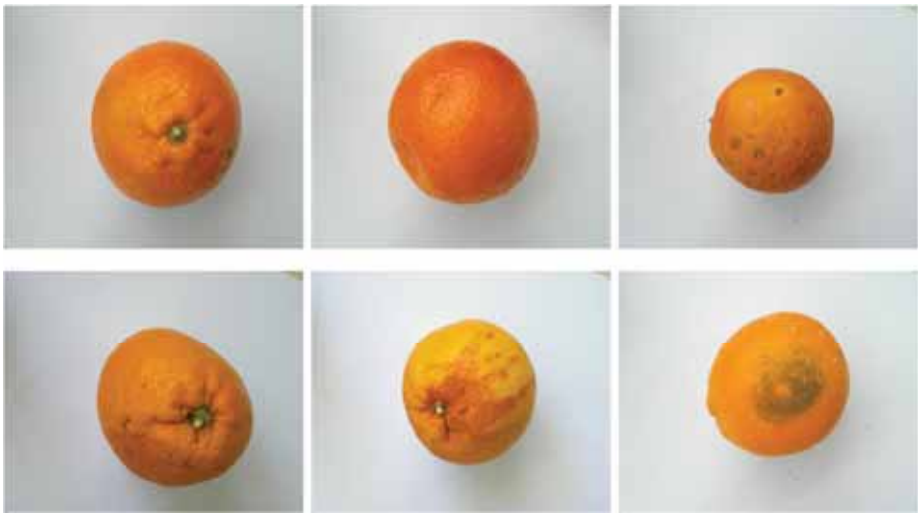

Fig. 1. Different sample of oranges used for this work. From left to right and top to bottom: Two normal oranges, an orange with several surface defects, a morphology defect, an orange with color defect, and an orange affected by a black mould.

The objective of this study was to investigate the applicability of a method for detection of external defects and an automatic orange's classification system.For this purpose, the development of a classifier based on textural features of images, captured with a digital camera, was evaluated.

The proposed technique is very robust and can identify specific defects like: surfacedefect, morphological defect, color defect, black mould or recognise a normal fruit (see Fig. 1). In fact, our RBPNN model is able to correctly attribute the samples to the correct defect groups with an overall error of 2.75%.

2. Fruit classification technique

In previous years, several types of image analysis techniques are applied to analyse the agricultural images such as fruits and vegetables, for recognition and classification purposes. The most popular analysis techniques that have been used for both recognition

and classifications of two dimensional (2D) fruit images are color-based and texture-based analysis methods.

2.1. *Fruit classification based on shape*

Shape based classification of fruits is based on various features like area, perimeter, major axis length and minor axis length. For calculating shape features an RGB image is converted into a gray scale image. After conversion into gray scale, the image represents a luminance intensity scale. There is a difference in intensity values for an object to be classified and its background, hence a threshold value is used to separate an object from its background. According to this threshold value, a gray scale image is converted into a binaryimage in which the value greater than the threshold is 1 and the value lower than the threshold is 0. With the help of this binary image different shape features are computed. The most common shape features are computed from the image area, perimeter, major axis length and minor axis length.

2.2. *Fruit classification based on color*

RGB color space is converted into another color space such as HSV and for all the converted color space values, the mean and standard deviation are calculated. Each fruit image gives different values of mean and standard deviation, therefore assisting its classification.

2.2.1. *HSV Color Space*

HSI stands for hue, saturation and intensity. Then, for an image thecolor attribute is given by hue and the amount by which the pure color is diluted by whiteis given by saturation. The RGB components are separated from the original image, and the Hue (H), Saturation (S) and Intensity (I) components are extracted from RGB components. Equations (1), (2) and (3) are used to evaluate Hue, Saturation and Intensity of the image samples.

$$\mathrm{H} = \begin{cases} \theta & \mathrm{B} \le \mathrm{G} \\ 360 - \theta & \mathrm{B} \ge \mathrm{G} \end{cases} \tag{1}$$

$$\theta = \cos^{-1}\left\{\frac{1}{2}\left(\frac{\lfloor (R-G)+(R-B) \rfloor}{\lfloor (R-G)^2+(R-B)\sqrt{G-B} \rfloor}\right)\right\}$$

The saturation component is given by:

$$S = 1 - \left(\frac{3}{R+G+B}\right)\left[\min(R,G,B)\right] \tag{2}$$

$$I = \frac{1}{3}\left(R+G+B\right) \tag{3}$$

2.3. *Fruit classification based on texture*

One of the simplest approaches for describing texture is to use the statistical moments of the gray level histogram of the image. Commonly used histogram statistics include range, mean, geometric mean, harmonic mean, standard deviation, variance, and median. Measures of texture computed using histograms suffer from the limitation that they carry no information regarding the relative position of the pixels with respect to each other. One way to bring this type of information into the texture analysis process is to consider not only the distribution of the intensities but also the positions of pixels with equal or nearly equal intensity values.Gray level co-occurrence matrix is used to calculate different texture features [Keller,*et al*(1989)].

Texture is classified by the spatial distribution of gray levels in a neighbourhood. It also helps in surface and shape determination. There are two methods that can be used to calculate the texture feature of an image. One is the statistical texture analysis; the other is the structure of texture analysis. The former is the most conventional. Statistical texture analysis methods include spatial autocorrelation method, Fourier power spectrum method, Co-occurrence matrix method, gray level difference statistics method and trip length statistics method. Color mapping co-occurrence matrix (CMCM) is used to extract the texture information from a skin image. Gray level co-occurrence matrix (GLCM) is used to extract texture features in an image. It represents the form of tabulation which contains different combinations of pixel brightness values (gray levels) that occurs in an image. To calculate the different texture features like entropy, energy, homogeneity and dissimilarity, a gray level co-occurrence matrix is created.

Given an image I, of size $N \times N$, the co-occurrence, matrix P can be defined as:

$$P(i, j) = \sum_{x=1}^{N} \sum_{y=1}^{N} \begin{cases} 1, & \text{if } I(x, y) = i \text{ and } I(x + \Delta_x, y + \Delta_y) = j \\ 0, & \text{otherwise.} \end{cases} \quad (4)$$

Here, the offset (Δ_x , Δ_y), is specifying the distance between the pixel-of-interest and its neighbour. Note that the offset (Δ_x , Δ_y) parameterization makes the co-occurrence matrix sensitive to rotation. To avoid this problemwe set$\Delta_x = \Delta_y = d$. The texture featuresbased on co-occurrence matrix can be calculated by using the following equations.

$$p_x(i) = \sum_{j=1}^{N_g} p(i, j), p_y(j) = \sum_{i=1}^{N_g} p(i, j) \quad (5)$$

where $p(i, j)$ is the (i, j)-th entry in normalized co-occurrence matrix; $N_g$denotes the dimension of co-occurrence matrix (number of gray levels), and $p_x(i)$ and $p_y(j)$ are the marginal probabilities

$$\mu_x = \sum_{i=1}^{N_g} i p_x(i), \mu_y = \sum_{i=1}^{N_g} i p_y(i) \quad (6)$$

μ is the mean of x (μ_X) and y (μ_Y);

$$\sigma_x = \left(\sum_{i=1}^{N_g} p_x(i)(i-\mu_x)^2 \right)^{1/2}, \sigma_y = \left(\sum_{i=1}^{N_g} p_y(i)(i-\mu_y)^2 \right)^{1/2} \quad (7)$$

and $\sigma_X$and σ_Y are the standard deviations of $p_X$and $p_Y$respectively.

Since the use of the co-occurrence matrices leads to a course of dimensionality, in literature are used some statistical features introduced by Haralick [Haralick,*et al*(1973)]. These features are generated by calculating the features for each one of the co-occurrence matrices obtained by using the directions 0°, 45°, 90°, and 135°.

In our approach we will construct a feature space, for the classification of the fruits, by using the following standard statistical descriptors:

Angular Second Moment: Consists of the sum of the squared elements in the co-occurrences matrix taken by pairs

$$ASM = \sum_{i=1}^{N_g} \sum_{j=1}^{N_g} \left| p(i,j) \right|^2 \quad (8)$$

Contrast: The global contrast of the image (also known as variance or *inertia*) measures the contrast intensity between a pixel and its neighbours

$$Contrast = \frac{1}{(N_g - 1)^2} \sum_{i=1}^{N_g} \sum_{j=1}^{N_g} (i-j)^2 \, p(i,j) \quad (9)$$

Correlation: Measures the relation of a pixel and its neighbours. The degree in which if the gray level of a pixel increases, its neighbour also increases

$$Correlation = \frac{\sum_{i=1}^{N_g} \sum_{j=1}^{N_g} (i-\mu_x)(i-\mu_y) \, p(i,j)}{\sigma_x \sigma_y} \quad (10)$$

Gradient Module: Is a measure of the degree of asymmetry of a distribution around the mean. It is obtained by calculating the third central moment of the distribution. If the

obtained value is zero, it means that it is centered (like the normal distribution). If it is positive, it is asymmetrical to the right, and if it is negative, to the left

$$GM = \sum_{i=1}^{N_g} \sum_{j=1}^{N_g} p(i, j) f(i)^2$$
$$f(i) = i - N_g + 1 \qquad (11)$$

Intensity symmetry: Is a measure of the variation of the texture if the grey levels are reversed

$$IS = 1 - \sum_{i,j}^{N_g} \left| p(i, j) - p(N_g - 1 - i, N_g - 1 - j) \right| \qquad (12)$$

3. Classification process of the orange defects.

The European Union defines three quality classes (*extra*, *class I* and *class II*) for the fresh oranges with the tolerances of 5% and 10% by number or weight, respectively. The oranges in the *extra* class must be of superior quality with no defects or irregularity in shape, whereas the *class I* and *class II* can contain defects up to 1 $cm^2$and 2.5 cm^2, respectively. All defect types in oranges contribute roughly equally to the final grading decision as local color, structural or textural variation of oranges.

In our classifier the defect detector uses a set of masks to recognise regions on the orange image. The defect is characterised by a discontinuity in the skin pigmentation.

The features extracted from the orange images in either spatial or frequency domain can be used for classification. The external surface quality is directly related to the marketing and sales. Our automatic grading system can significantly improve the accuracy and consistency, while at the same time eliminating the subjectivity of manual inspection. The defects that we are able to detect on the external surface are caused by two reasons:

- Pre-harvest and Post-harvest diseases, like: diplodia and phomopsis stemend rot, splitting, pitting, green and blue mold, sour and brown rots, anthracnose, etc.
- Mechanical damages during transportation.

The defects on the orange fruit are characterised by different textures. Among various textures, we categorised defect types like:

- Pitting, which is caused by mechanical damage or reduced gas exchange during transportation. Pits can coalesce to form irregular patches and brown to black blemishes.

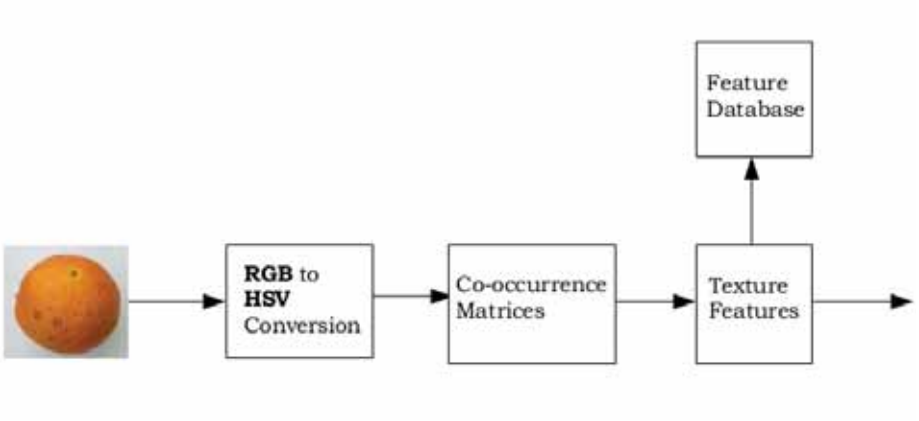

Fig. 2. Features extraction.

- Splitting is caused by the inability of the outer skin to hold the weight of the whole fruit. The outer skin of the citrus fruit splits and the inner pulp gets exposed. The defective region is usually brighter when compared with the normal skin.

For the research we used a data set obtained after processing high quality orange images and defective quality orange images (640 by 480 pixels), for a total of 400 acquired images that are obtained by rotating and rearranging fruit samples.

In order to improve the quality of an image, operations need to be performed on it to remove or decrease degradations suffered by the image during its acquisition. The captured images are suffering from illumination variations, due to specular reflection.

The reflected parts become full white and also the shadows; these are the main challenges in defect detection. We employ median filtering to normalize the uneven distribution of light and to suppress noise. The median is much less sensitive than the mean to extreme values (called outliers). Median filtering is therefore better able to remove these outliers without reducing the sharpness of the image. The median filter technique allowed the edges to be preserved while filtering out the peak noise.

4. Proposed technique for orange feature extraction

The feature extraction process is illustrated in Fig. 2.

The proposed feature extraction technique shown in Fig.2, need a change in the color space of the images, in order to obtain one channel containing the luminance information and two other channels containing chrominance information. The HSV representation is often selected for its invariant properties.

Fig. 3. An orange with some surface defects and the segmentation preprocessing result: the background is removed in order to analyze the orange surface only.

The foreground region (orange) then can be segmented out from the background by using the Hue and Saturation histograms of the image. In order to extract the features, thepictures have been firstly segmented and the background removed. This latter stage is very fast and its computational weight can be neglected, since it only uses the saturation histogram and a saturation threshold having value 0.049 (this value has been computed as the average local minima with respect to the overall image set, point between the two principal peaks of the saturation histogram in order to allow us to obtain a fast and suitable image segmentation). Fig. 3 shows an orange with several surface defects and the segmentation result, while Fig. 4 shows the saturation and hue histogram of the same orange.

In addition to the segmentation using its HSV representation, we use color histogram and GLCM (Gray level co-occurrence matrix) to find quality classes corresponding to the orange qualities. For practical applications, the original input variables are typically preprocessed to transform them into some new space of variables where the pattern recognition problem will be easier to solve. This preprocessing stage is called *feature extraction*, see [Bishop(2006)]. Preprocessing is performed in order to speed up computation and improve the classification performance. We then selected useful features that are fast to compute and allow easy discrimination [Nowak,*et al*(2015)],[Napoli et al. (2015a)],[Napoli and Tramontana (2015b)].

A feature set suitable for the classification should be insensitive to significant translations and have a very low correlation. Therefore, we base the extraction of features on the array of co-occurrence matrix, see [Arvis, *et al.* (2011)]. Co-occurrence matrix is a single level dependence matrix that contains relative frequencies of two coordinate elements separated by a distance *d*. As you move from one pixel to another on the image, entries of the initial and final pixels become thecoordinates of the co-occurrence matrix to be incremented, which in the end will represent structural characteristics of the image.

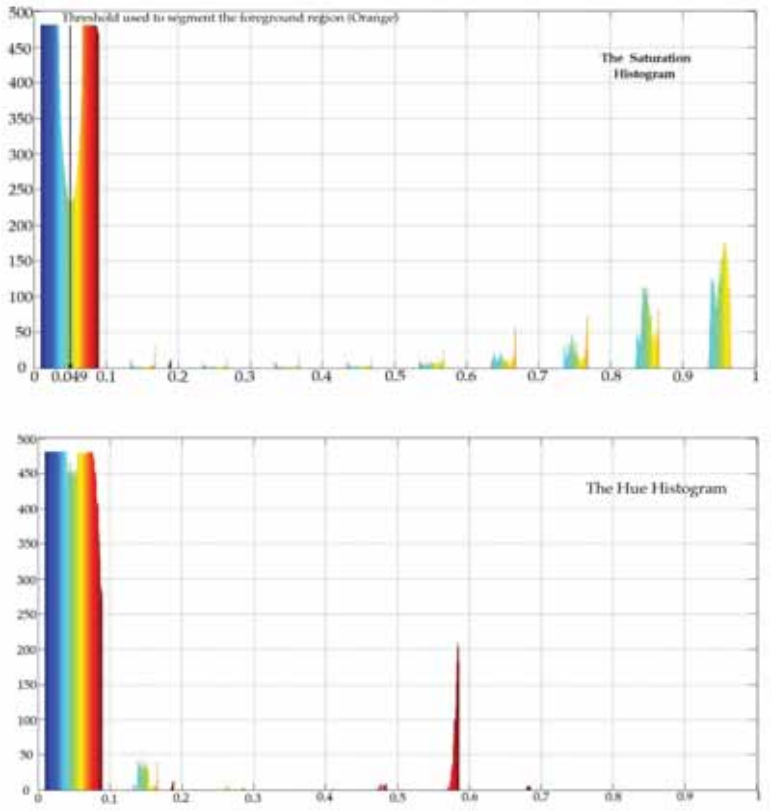

Fig. 4. The saturation (above) and hue (below) histogram related to the orange depicted in Fig. 2. The result shown in Fig. 2 is obtained by thresholding the saturation histogram shown here.

Therefore, moving in different directions and distances on the image will lead to different co-occurrence matrices. For each image we have calculated three co-occurrence matrices: one for each channel Hue, Saturation, Value. The obtained features represent the area of the orange, the background (the contrast, like gray level uniformity), gray level correlation between neighbours, sum average and sum variance. The features were calculated from the normalised co-occurrence matrix for $d = 1$ and four main directions: 0°, 45°, 90° and 135°.

In our case four angles, namely 0°, 45°, 90°, and 135°, are considered as well as a predefined distance of one pixel, in the formation of the co-occurrence matrices. Therefore, we have formed four co-occurrence matrices. A contrast equation (9) is used to calculate four parameters respectively, 0°, 45°, 90°, 135°. Then a fifth parameter is associate to each channel: the average value of the channel itself. This permits us to obtain five different feature for each channel, with an overall of fiftheen features associated to each image.

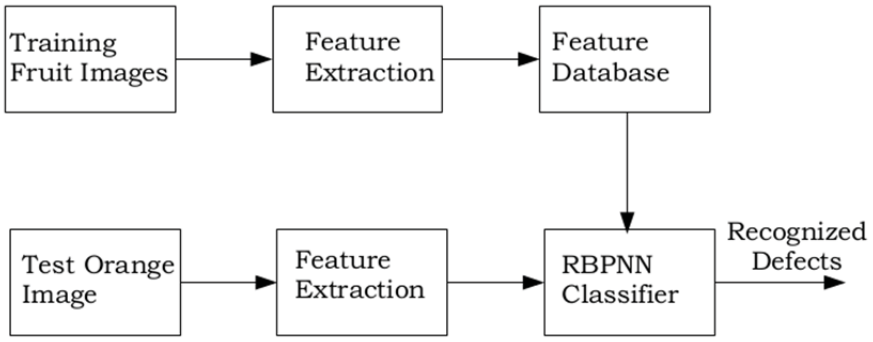

Fig. 5. Orange defects recognition System.

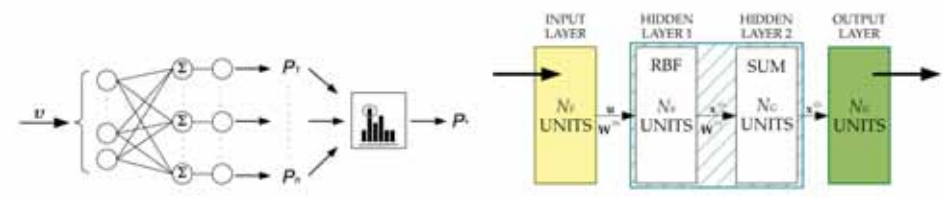

Fig. 6. A representation of our Radial Basis Probabilistic Neural Network (RBPNN) with maximum probability selector module. On the right the RBPNN layers model: NF is the number of features, NS is the number of samples and NG is the desired number defects to identify.

This feature set extraction has a low dimensionality and a good discriminatory power. The features are extracted and fed into the Artificial Neural Network (ANN) classifier for defect classification. Training, testing, and validation of neural networks are performed using sample images [Woźniak, *et al.* (2015b)].The block diagram of the proposed orange defects classification method is shown in Fig. 5.

5. The selected RBPNN

The proposed RBPNN (Fig. 6) is an implementation of a statistical algorithm called kernel discriminant analysis, see [Ripley (1996)], in which the operations are organised into a multi-layered feed-forward network with four layers: an input layer, a pattern layer (the first hidden layer), a summation layer (the second hidden layer), and an output layer. Basically a RBPNN consists of an input layer, which represents the input pattern or feature vector. The input layer is fully interconnected with the hidden layer, which

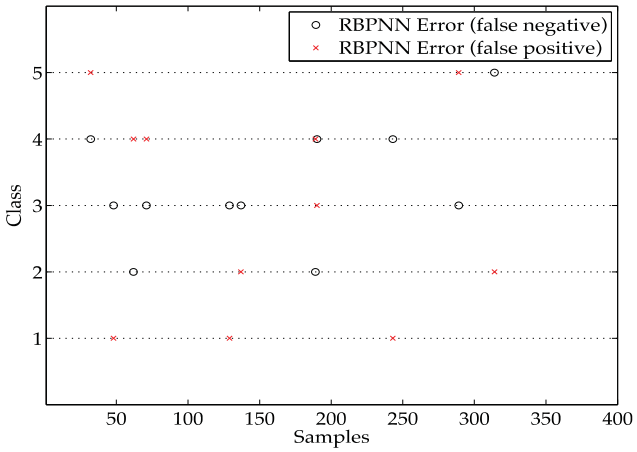

Fig. 7. The identification'sresults obtained by our system at validation time: the circles show the effective class of the oranges, while the crosses show the identification output given by the implemented system.

consists of the example vectors (the training set for the PNN [Napoli, et. al. (2015a)], [Bonanno, et. al. (2014a)]).

One other important element of the RBPNN is the outputlayer and the determination of the class for which the input layer fits. This is done through a winner-takes-all approach. The output class node with the largest activation represents the winning class. While the class nodes are connected only to the example hidden nodes for their class, the input feature vector connects to all examples and therefore influences their activations. It is therefore the sum of the example vector activations that determines the class of the input feature vector. In RBPNN algorithm, calculating the class-node activations is a simple process. For each class node, the example vector activations are summed, which are the sum of the products of the example vector and the input vector. Input neurons are used as distribution units that supply the same input values to all the neurons in the first hidden layer (such neurons are called *pattern units*). Each pattern unit performs the dot product $(\cdot)$ of the input pattern vector $\mathbf{u}$ by a weight vector $\mathbf{W}^{(0)}$. Then each pattern unit performs a nonlinear operation on the result. This nonlinear operation gives output $\mathbf{x}^{(1)}$that is handed to the following summation layer. While the common sigmoid function is used for a standard FFNN, in our BPTA for presented PNN the activation function is exponential. Therefore for the j neuron the output is where σ represents the statistical distribution spread

$$x_j^{(1)} \propto \exp\left(\frac{\left\|W^{(0)} \cdot u\right\|}{2\sigma^2}\right) \quad (13)$$

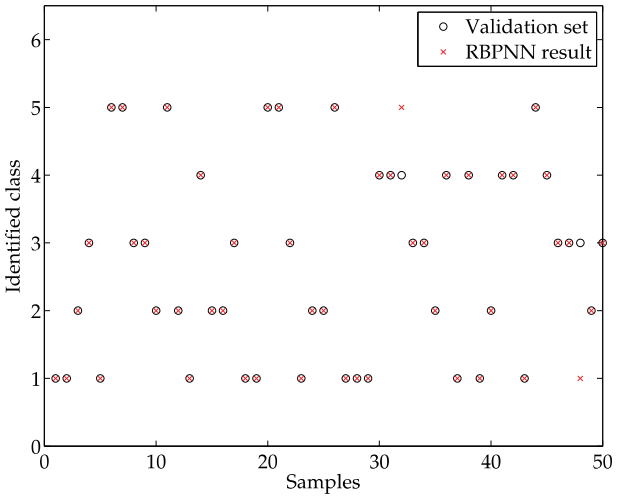

Fig. 8.The identification'serrors of the proposed system:the circles identify the false negative results, while the crosses the false positive results.

In the proposed model, while preserving the PNN topology [Bonanno,*et. al.* (2012)], in order to obtain RBPNN capabilities, the activation function has been substituted with a Radial Basis Function (RBF). Moreover, there is the equivalence between the $\mathbf{W}^{(0)}$vector of weights and the centroids vector of RBNN, which in our classifier are computed as the statistical centroids of all the given input sets. We name ρ the chosen RBF, then the new output of the first hidden layer for the *j* neuron is:

$$x_j^{(1)} \propto \rho\left(\frac{\left\|u - W^{(0)}\right\|}{\beta}\right) \quad (14)$$

where β is the distribution shape control parameter, similar to σ used in [Woźniaket al., (2014c)].

The second hidden layer in our RBPNN is a PNN. It computes weighted sums of received values from the preceding neurons. This second hidden layer is called summation layer with the output of the *k* summation unit

$$x_k^{(2)} = \sum_j W_{jk} x_j^{(1)} \quad (15)$$

where $\mathbf{W}_{jk}$represents the weight matrix. Such weight matrix consists of a weight value for each connection from the j pattern unit to the k summation unit. The summation units work as the neurons of a linear perceptron network. The training for the output in the applied model is performed similarly to RBNNs, but also initializing the centroids with a k-means algorithm, and then proceeding by adjusting weights, centroids, and spread coefficients, with a standarda back propagation algorithm as in [Wozniak et al. (2015b)] and [Wozniak et al. (2015c)].

6. Experimental results and conclusions

In our RBPNN classifier, defects were grouped into categories: surface defect as bruises (class 2), morphological defects (class 3), slight color defects (class 4), black mould (class 5) and a category of good fruit (class 1). The proposed classifier has been tested on a large number of image orange samples collected in a database (see Fig.7).

Table 1. . A brief statistical analysis of the results by class.

Class	**Fruit condition**	**Number of samples**	**False negative**	**False positive**
1	Normal fruit	85	0	3
2	Surface defect	97	2	2
3	Morphological defect	71	5	1
4	Color defect	83	3	3
5	Black mould	64	1	2
Overall Classification		**Number of samples**	**Correctly classified**	**Overall error**
		400	389	2.75%

This section shows 400 samples of different defects of fresh orange surface include stab wounds, bruise, abrasion, sunburn, injury, hail damage, cracks and insect pest damage and good oranges. Fig. 8 shows the different recognitions. Our RBPNN model is able to correctly attribute the orange samples to the correct defect groups with an overall error of 2.75% (see Table 1). The error has been evaluated comparing the classification results with the ground truth results provided by an expert human operator.

The proposed solution enabled us to obtain a fast and efficient automatic classification system for fruits defects.

Although in an early stage of development, still such a system could be proposed on large scale for industrial applications, as well as for an implementation into programmable hardware.

References

Arvis, V. *et al.* (2011): Generalization of the co-occurrence matrix for colour images: application to colour texture classification. Image Analysis & Stereology, **23**(1), pp. 63–72.

Anami, B. S.; Savakar, D. S. (2009): Effect of foreign bodies on recognition and classification of bulk food grains image samples. J. Appl. Comput. Sci., **6**(3), pp. 77–83.

Bishop, C. M. (2006).*Pattern recognition and machine learning*, Springer, New York.

Ripley, B. D. (1996).*Pattern recognition and neural network,* Cambridge University Press.

Bonanno, F.; Capizzi, G.; Lo Sciuto, G.; Napoli, C.; Pappalardo, G.; Tramontana, E. (2014a): A novel cloud-distributed toolbox for optimal energy dispatch management from renewables in igss by using wrnn predictors and gpu parallel solutions. In IEEEInternational Symposium on Power Electronics, Electrical Drives, Automation and Motion (SPEEDAM), pp. 1077–1084.

Bonanno, F.; Capizzi, G.; Coco, S.; Napoli, C.;. Laudani, A; Lo Sciuto, G. (2014b): Optimal thicknesses determination in a multilayer structure to improve the spp efficiency for photovoltaic devices by an hybrid fem–cascade neural network based approach. In Proceedings ofIEEEInternational Symposium on Power Electronics, Electrical Drives, Automation and Motion (SPEEDAM), pp. 355–362.

Bonanno, F.; Capizzi, G.; Napoli, C. (2012): Some remarks on the application of rnn and prnn for the charge-discharge simulation of advanced lithium-ions battery energy storage. In Proceedings ofIEEEInternational Symposium on Power Electronics, Electrical Drives, Automation and Motion (SPEEDAM), pp. 941-945.

Capizzi, G; Bonanno, F.; Napoli, C. (2011): Recurrent neural network- based control strategy for battery energy storage in generation systems with intermittent renewable energy sources. In Proceedings ofIEEE international conference on clean electrical power (ICCEP), pp. 336– 340.

Damasevicius, R., Toldinas, J., Grigaravicius, G. (2013): Modelling Battery Behaviour Using Chipset Energy Benchmarking, Elektronika Ir Elektrotechnika, **19(6)**, pp. 117-120.

Ferdowsi, S., Voloshynovskiy, S., Kostadinov, D., Korytkowski, M., Scherer, R. (2015): Secure Representation of Images Using Multi-layer Compression. Lecture Notes in Artificial Intelligence – ICAISC'2015, **9119**, pp. 696-705.

Haralick, R. M.; Shanmugam, K.; Dinstein, I. H. (1973): Textural features for image classification. IEEE Transactions on Systems, Man and Cybernetics,**6**, pp. 610–621.

Horzyk, A. (2015): Innovative types and abilities of neural networks based on associative mechanisms and a new associative model of neurons. Lecture Notes in Artificial Intelligence – ICAISC'2015, **9119**, pp. 26–38.

Horzyk, A. (2014): How does generalization and creativity come into being in neural associative systems and how does it form human-like knowledge?. Neurocomputing, **144**, pp. 238–257.

Keller, J. M.; Chen, S.; Crownover, R. M. (1989): Texture description and segmentation through fractal geometry. Computer Vision, Graphics, and Image Processing, **45**(2), pp. 150–166.

Korytkowski, M., Rutkowski, L., Scherer, R. (2016): Fast image classification by boosting fuzzy classifiers. Information Sciences, **327**, pp. 175-182.

Kostadinov, D., Voloshynovskiy, S., Ferdowsi, S., Diephuis, M., Scherer, R. (2015): Supervised Transform Learning for Face Recognition. Lecture Notes in Artificial Intelligence – ICAISC'2015, **9119**, pp. 737-746.

Kubanek, M.; Smorawa, D.; Holotyak, T. (2015): Feature extraction of palm vein patterns based on two-dimensional density function. Lecture Notes in Artificial Intelligence – ICAISC 2015, **9120**, pp. 101–111.

Leemans, V.; Magein, H.; Destain, M. F. (1998): Defects segmentation on golden delicious apples by using colour machine vision. Computers and Electronics in Agriculture, **20**(2), pp. 117–130.

Miller, W.; Throop, J.; Upchurch, B. (1998): Pattern recognition models for spectral reflectance evaluation of apple blemishes. Postharvest Biology and Technology, **14**(1), pp. 11–20.

Nakano, K. (1997): Application of neural networks to the color grading of apples. Computers and electronics in agriculture, **18**(2), pp. 105–116.

Napoli, C; Pappalardo, G.; Tramontana, E.; Nowicki, R.; Starczewski, J.; Woźniak M. (2015a): Toward work groups classification based on probabilistic neural network approach. Lecture Notes in Artificial Intelligence – ICAISC'2015, **9119**, pp. 79–89.

Napoli C and Tramontana E, (2015b): An Object-Oriented Neural Network Toolbox Based on Design Patterns, Communications in Computer and Information Science - ICIST'2014, **538,** pp. 388-399.

Nowak, B.; Nowicki, R.; Woźniak, M.; Napoli, C. (2015): Multi-class nearest neighbour classifier for incomplete data handling. Lecture Notes in Artificial Intelligence – ICAISC'2015,**9119**, pp. 469– 480.

Połap, D., Woźniak, M.; Napoli C, Tramontana E (2015a): Is Swarm Intelligence Able to Create Mazes?. International Journal of Electronics and Telecommunications, **61(4)**, pp. 305–310.

Połap, D., Woźniak, M.; Napoli C, Tramontana E (2015b): Real-Time Cloud-based Game Management System via Cuckoo Search Algorithm. International Journal of Electronics and Telecommunications, **61(4)**, pp. 333–338.

Pukish, M. S. ; Rózycki, P.; Wilamowski, B. M. (2015): Polynet: A polynomial-based learning machine for universal approximation. IEEE Trans. Industrial Informatics, **11**(3), pp. 708–716.

Reiner, P.D.; Wilamowski, B.M. (2015): Efficient incremental construction of RBF networks using quasi-gradient method. Neurocomputing, **150**, pp. 349–356.

Savakar, D. G.; Anami, B. S. (2009): Recognition and classification of food grains, fruits and flowers using machine vision. International Journal of Food Engineering, **5**(4), pp. 112-124.

Swiechowski, M., Mandziuk, J. (2014): Self-Adaptation of Playing Strategies in General Game Playing. IEEE Trans. Comput. Intellig. and AI in Games, **6(4)**, pp. 367-381.

Waledzik, K., Mandziuk, J. (2014): An Automatically Generated Evaluation Function in General Game Playing. IEEE Trans. Comput. Intellig. and AI in Games, **6(3)**, pp. 258-270.

Wen, Z.; Tao, Y. (2000): Dual-camera nir/mir imaging for stem-end/calyx identification in apple defect sorting. Transactions of the ASAE, **43**(2) , pp. 449–452.

Woźniak, M.; Połap, D. (2015a): On some aspects of genetic and evolutionary methods for optimization purposes. International Journal of Electronics and Telecommunications, **61(1)** , pp. 7–16.

Woźniak M, Napoli C, Tramontana E and Capizzi G, Lo Sciuto G. (2015b): A multiscale image compressor with RBFNN and Discrete Wavelet decomposition, In International Joint Conference on Neural Networks – IJCNN'2015 , pp. 1219–1225.

Woźniak M, Polap D, Nowicki RK, Napoli C, Pappalardo G and Tramontana E. (2015c): Novel approach toward medical signals classifier, In International Joint Conference on Neural Networks – IJCNN'2015, pp. 1924–1930.

Woźniak M., Polap D., Nowicki R. K., Gabryel, M., Napoli C, Tramontana E (2015d): Can We Process 2D Images Using Artificial Bee Colony?. Lecture Notes in Artificial Intelligence – ICAISC'2015**9119**, pp. 660-671.

Woźniak M., Połap D. (2014a): Basic concept of cuckoo search algorithm for 2D images processing with some research results : An idea to apply Cuckoo search algorithm in 2D images key-points search. In SIGMAP 2014 - Proceedings of the 11th International Conference on Signal Processing and Multimedia Applications, Part of ICETE 2014 - 11th International Joint Conference on e-Business and Telecommunications, pp. 157-164.

Woźniak, M.; Marszałek, Z. (2014b): An idea to apply firefly algorithm in 2D images key-points search. Communications in Computer and Information Science - ICIST'2014, **465**, pp. 312–323.

Woźniak, M. (2014c): Fitness function for evolutionary computation applied in dynamic object simulation and positioning. In IEEE Symposium Series on Computational Intelligence - CIVTS IEEE Symposium on Computational Intelligence in Vehicles and Transportation Systems, 2014, pp. 108–114.

Zhang, L.; Yang, Q.; Xun, Y.; Chen, X.; Ren, Y.; Yuan, T.; Tan, Y.; Li, W. (2007): Recognition of greenhouse cucumber fruit using computer vision. New Zealand Journal of Agricultural Research, **50**(5), pp. 1293–1298.